Enzymatic Ligation Creates Discrete Multi-Nanoparticle Building Blocks for Self-Assembly

Shelley A. Claridge, Alexander J. Mastroianni, Yeung B. Au, Huiyang W. Liang, Christine M. Micheel, Jean M. J. Fréchet, and A. Paul Alivisatos*.*

Department of Chemistry, University of California, Berkeley, California 94720-1460 and Division of Materials Science, Lawrence Berkeley National Laboratory, Berkeley, California 94720

AUTHOR EMAIL ADDRESS frechet@berkeley.edu, alivis@berkeley.edu

RECEIVED DATE (to be automatically inserted after your manuscript is accepted if required according to the journal that you are submitting your paper to)

TITLE RUNNING HEAD Enzymatic Ligation of Nanoparticle Conjugates

CORRESPONDING AUTHOR FOOTNOTE frechet@berkeley.edu Tel (510) 643-3077 Fax (510) 643-3079 alivis@berkeley.edu Tel (510) 643-7371 Fax (510) 642-6911

ABSTRACT Enzymatic ligation of discrete nanoparticle–DNA conjugates creates nanoparticle dimer and trimer structures in which the nanoparticles are linked by single-stranded DNA, rather than double-stranded DNA as in previous experiments. Ligation is verified by agarose gel and small-angle X-ray scattering. This capability is utilized in two ways: first to create a new class of multiparticle building blocks for nanoscale self-assembly; second to develop a system which can amplify a population of discrete nanoparticle assemblies.

KEYWORDS GOLD, NANOPARTICLE, NANOCRYSTAL, DNA, ENZYME, LIGASE, LCR, BIOCONJUGATE, SELF-ASSEMBLY, SAXS.

MANUSCRIPT TEXT

INTRODUCTION

Recent research in nanoassembly has demonstrated that DNA may be used to control the self-assembly of inorganic nanoparticles into designed functional materials,[1-3] by exploiting the sequence-specific base pairing that governs its native assembly. In living systems, DNA serves as genetic information, a function so vital that nature has developed a multitude of enzymes to control its replication, correct errors in DNA sequences, and even destroy foreign DNA that enters a cell.[4] Certain DNA-manipulating enzymes, such as restriction enzymes[5,6] and polymerases[7], have also proven to be active on DNA–nanoparticle conjugates, suggesting that it may ultimately be possible to leverage the library of DNA-active enzymes to create more complex self-assembled nanomaterials and perhaps even to enable such functions as self-replication and error correction in a materials context. Nature's enzymatic toolkit is an important and underutilized asset in DNA-mediated self-assembly of functional materials.

Here, we show that DNA ligases, which seal single-stranded nicks in double-stranded DNA (dsDNA), can also operate on DNA–gold monoconjugates, structures in which a single strand of thiolated DNA is bound to a gold nanocrystal. Previous work has demonstrated that large networks may be formed through ligation of nanoparticles whose surfaces are conjugated with large numbers of DNA strands.[8,9] In this work, ligation causes formation of a covalent bond between discrete nanoparticle–DNA conjugates, creating a new type of building block for self-assembly.

These new nanoassembly components offer a number of advantages. In these building blocks, multiple gold nanoparticles are linked by single-stranded DNA (ssDNA) (Scheme 1), and thus retain the sequence-specific targeting ability of the ssDNA linker. This contrasts with previous experiments, in which DNA–gold dimers have been formed by hybridization of two DNA–gold monoconjugates[10] and thus are intrinsically linked by double-stranded DNA (dsDNA). Additionally, since particles within

these new ligated building blocks are covalently linked the particles will remain connected under conditions such as high temperature or low salt concentrations which would cause disassembly in structures formed by base pairing. The ability to pre-form multiparticle components for later assembly is also a powerful asset in that it allows preformed components to be purified individually, which may ultimately facilitate assembly into complex structures such as nanoscale devices.

Scheme 1. Overview of ligation process. Nanoparticle–DNA monoconjugates are hybridized to a ssDNA template and enzymatically ligated to create gold nanoparticle dimers. Template strand is then removed, leaving two nanoparticles connected by ssDNA.

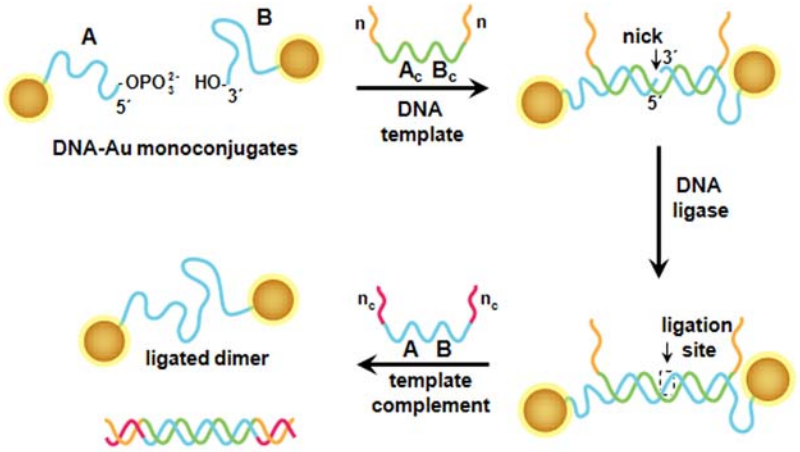

The capability to operate with DNA-active enzymes on discrete DNA–nanocrystal conjugates also opens the door to the use of enzymatic chain reaction technology[11,12] to apply amplification in nanomaterial construction. Similar to the manner in which PCR can be used to amplify tiny amounts of a sequence of DNA bases, we use a ligase chain reaction (LCR)[12] to amplify the quantity of ligated DNA–gold dimer structures starting from small amounts of template. Since the ligation process we describe also effectively 'polymerizes' the nanoparticle conjugates to make short chains of nanoparticles, this can be considered to be roughly equivalent to PCR for nanoparticles – here we demonstrate formation of the shortest possible chain (two particles). Optimization of the amplification process could potentially allow construction of longer chains consisting of an arbitrary 'sequence' of nanoparticles, which could then act as the template for formation of a 'complementary' sequence of nanoparticles bioconjugates in order to engineer properties such as plasmonic coupling[13] between pairs of nanoparticles on the chain. It should be noted that the efficiency of such a process would be limited

relative to true PCR, since it relies on the action of a DNA ligase, which is typically less efficient than a DNA polymerase. However, we demonstrate that our modified ligase chain reaction protocol can produce quantities of DNA–gold structures practical for self-assembly experiments.

Ligation of discrete gold nanoparticle monoconjugates bearing a single strand of DNA offers substantial rewards in terms of control over self-assembly, but levies additional requirements on the substrates involved. DNA used for conjugation must be highly purified, as the ligation process depends critically upon the matching of 3′ and 5′ ends of DNA at the ligation site. The nanoparticle surface must be thoroughly passivated (in this case, by thiolated poly(ethylene glycol) ligands) in order to prevent aggregation in enzymatic buffers containing divalent cations. Further, monoconjugates purified via gel electrophoresis[14] are not ideal substrates as the samples may contain agarose impurities which are potent inhibitors of ligases.[15] We have used conjugates purified by anion exchange high performance liquid chromatography (AE-HPLC).[16]

RESULTS AND DISCUSSION

We first demonstrate successful hybridization and ligation as shown in Scheme 1 by analyzing reaction products in an agarose gel. Template removal is confirmed by small-angle X-ray scattering experiments. Multi-nanoparticle ssDNA building blocks are then self-assembled into complex nanoscale structures which are visualized by transmission electron microscopy. Finally, the ability to use an enzymatic exponential amplification method is explored as a means to amplify nanoparticle–DNA building block products.

Enzymatic Ligation Analyzed by Electrophoresis. Gold nanoparticles functionalized with a single strand of thiolated DNA were isolated using an AE-HPLC protocol previously described.[17] Enzymatic ligation using the T4 and *Taq* DNA ligase enzymes requires nicked double-stranded DNA, with the 5′ side of the nick phosphorylated.[12,18,19] For these experiments, gold nanoparticles were conjugated to 30-base sequences A and B, where A was purchased with a commercially available thiol modifier at its 3′ terminus and was 5′-phosphorylated, and B was 5′-thiolated (Scheme 1). Hybridization of conjugates A

and B to the 54-base template strand nA_cB_cn, in which the central 30 base A_cB_c sequence is complementary to conjugate sequences A and B, and the 12 bases on each end labeled 'n' do not hybridize, leaving a toehold for later removal of the template. Hybridization of conjugates and template created a nicked double-stranded hybrid, in which the 5′ side of the nick was the phosphorylated end of conjugate A. Addition of T4 DNA ligase and incubation at 16 °C for 30 min resulted in the formation of a covalent bond between the adjacent ends of conjugates A and B, creating a ligated dimer. Following ligation, the template strand was removed by addition of a DNA strand n_cABn_c complementary to the template.

When DNA–gold conjugate structures are analyzed by agarose gel electrophoresis, they give discrete bands corresponding to structures with increasing numbers of DNA strands and nanoparticles.[20] We have used electrophoresis to confirm dimer hybridization and enzymatic ligation. In an agarose gel, constructs travel at a rate that depends upon both their size and their charge, with smaller structures passing more readily through the pores in the gel. Thus, in the electrophoretic analysis (Figure 1), monoconjugates (lane 1) such as A and B migrate more quickly than hybridized nicked dimers (lane 2).

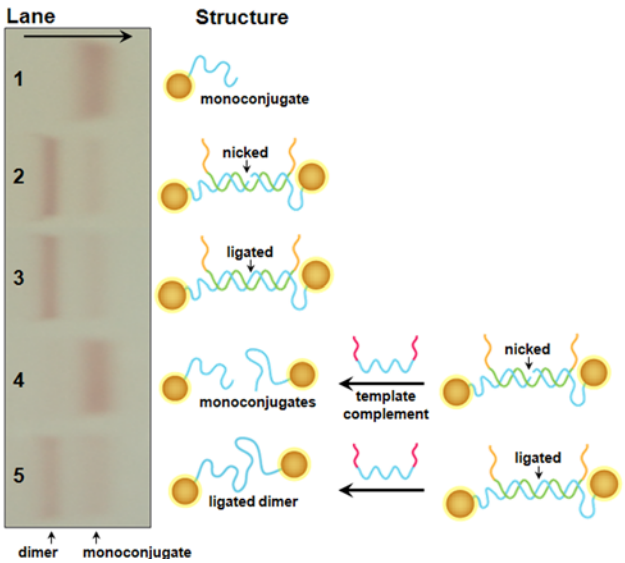

Figure 1. Electrophoretic analysis of monoconjugate ligation efficiency. Lane (1) monoconjugate B, (2) A and B plus ssDNA template, (3) A and B plus ssDNA template and T4 DNA ligase, (4) A and B plus ssDNA template and ssDNA complementary to template, (5) A, B, ssDNA template and ligase, with subsequent addition of ssDNA complementary to template.

Ligated dimers (lane 3) migrate at a similar rate to nicked dimers (lane 2), since the ligation process does not change the charge of the construct, and changes its size only insofar as the increased structural rigidity hinders progress through the porous gel. When unligated dimers such as those shown in lane 2 are mixed with the DNA strand complementary to the template strand, heated, and then slowly cooled, the template and its complement form a more stable hybrid than the template and the two conjugates. Thus, when the reaction products are analyzed in the gel (lane 4), the primary visible product is monoconjugate, rather than dimer.

However, when ligated dimers are mixed with the template complement strand, heated, and then cooled, the majority of the particles (71% by optical density analysis) still migrate as dimers in the gel (lane 5). While it is not clear, based on gel analysis alone, whether or not the template strand has been removed by its complement, lane 5 demonstrates successful ligation.

Analysis of Ligation and Template Removal by Small-Angle X-Ray Scattering (SAXS). In order to demonstrate that the template strand has indeed been removed through addition of its complement, leaving a ssDNA–nanoparticle dimer, the ligated dimers were analyzed by small-angle X-ray scattering. The relatively high electronic density of the gold nanoparticles and low electronic density of the DNA result in data which reflect the distribution of distances between the gold nanoparticles, without interference from the DNA between them. Previous studies[21,22] have elucidated the distances between nanoparticles connected by dsDNA, demonstrating that the interparticle distance reflects the length of the double-helical DNA linker.

SAXS is used to observe the structural difference between ligated nanoparticle dimers bound to the template, and ligated dimers from which the template has been removed (Figure 2a, similar to Figure 1, lanes 3 and 5). In both structures, the nanoparticles are separated by a 60-base DNA linker, but in the structure on the left, the central 30 bases of the linker are hybridized to the template, creating an approximately 10-nm double helix flanked by 15-base lengths of flexible ssDNA. In the structure on the right, after the template strand has been removed by addition of the template complement, the nanoparticles are separated by 60 bases of ssDNA. Since the persistence length of ssDNA (about 2 nm)

is much shorter than that of dsDNA (50 nm)[23], removal of the template is expected to lead to smaller interparticle distances.

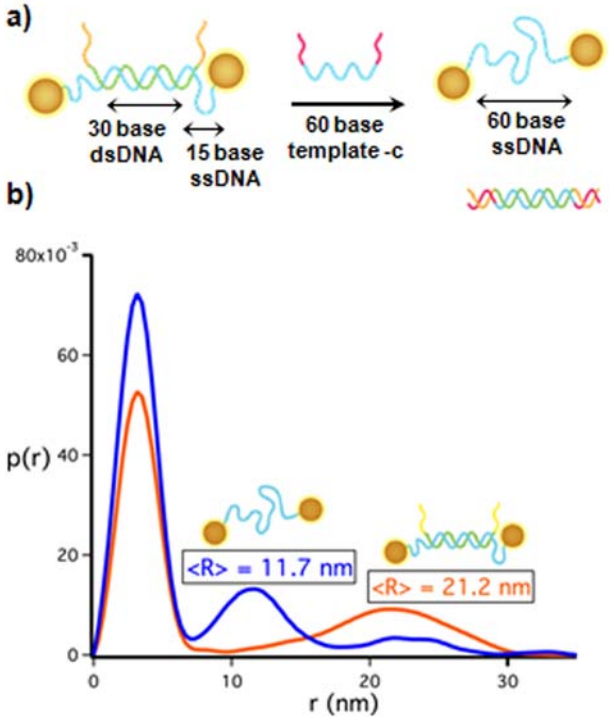

Figure 2. (a) Schematic of gold nanoparticle dimers connected by a single strand of ssDNA. (b) SAXS analysis shows a decrease in interparticle distance after removal of the template strand.

Figure 2b shows the effect of adding the template complement strand. When no template complement has been added (red trace), the SAXS pair distribution function shows a peak at 21.2 nm. When 2 equivalents of template complement are added and the sample is allowed to equilibrate for 24 hours (blue trace), a large peak appears at approximately 11.7 nm, with a small residual peak corresponding to structures from which the template has not been removed. What appears to be fine structure in the residual peak is actually noise from Fourier transformation, which is commonly observed for lower-intensity signals in this type of data.

Since the peaks at 11.7 nm and 21.1 nm are indicative of center-to-center distances between the nanoparticles, this would represent an end-to-end distance of approximately 16 nm for the DNA linker in the first case and 6 nm in the second case. Thus, although there is little difference in the migration of

the two structures in an agarose gel, distinctive characteristics in the pair distribution functions allow them to be differentiated unambiguously.

Self-Assembly of Ligated Nanoparticle Dimer and Trimer Structures. As a demonstration that ligated ssDNA dimers and trimers retain the targeting ability of their DNA linker, ligated dimers and trimers were synthesized and assembled to form nanoparticle tetramers and hexamers (Scheme 2). Tetramers were formed by hybridization of two complementary ligated dimers. To synthesize hexameric structures, nanoparticle diconjugates were first specifically ligated to two monoconjugates to form a symmetric strand of three nanoparticles connected by ssDNA. Two such complementary strands were synthesized and subsequently hybridized to yield a hexameric nanoparticle structure comprising three pairs of nanoparticles.

Figure 3a shows transmission electron micrographs of ligated nanoparticle dimers which have been incubated with template complement DNA to remove the ligation template strand. As a result, the two nanoparticles are attached to a length of ssDNA. Due to the decreased persistence length of ssDNA relative to dsDNA, the center-to-center interparticle distance varies widely, with an average of 20.9 ± 14.0 nm. It should be noted that the behavior of nanoparticle–DNA constructs dried on TEM grids differs markedly from their behavior in solution (Figure 2b), where the center-to-center distance of the same structures is 11.7 ± 2.8 nm. We presume that forces exerted on the sample while drying on the TEM grid override the entropic penalties associated with ssDNA stretching, resulting in larger interparticle distances as well as a larger distribution in the distances. The four particle pairs shown in Figure 3a demonstrate the extremes of both stretching (top and left pairs) and collapse (right pair), as well as the average case (bottom pair).

Scheme 2. Overview of self-assembly process. Nanoparticle dimers and trimers are created by enzymatic ligation of mono- or diconjugates as shown. Hybridization of complementary dimers or trimers leads to nanoparticle tetramers or hexamers.

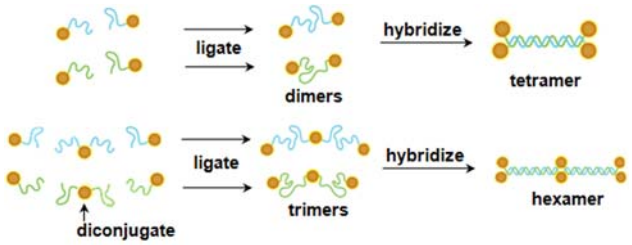

In Figure 3b, complementary ligated dimers have been hybridized to form nanoparticle tetramers, in which the increased structural rigidity provided by hybridization is evident. The majority of tetramers consist of two pairs of particles. If the long axis of the tetramer is taken to be the distance between the midpoints of the two pairs, the distribution is found to be 18.6 ± 2.6 nm, in agreement with the expected 20 nm length of a 60-base DNA double helix. The much smaller standard deviation reflects the increased rigidity of the structure.

The ligation strategy can also be extended to create more complex nanoscale building blocks. In Figure 3c, hybridization of two three-particle strands creates nanoparticle hexamers consisting of three pairs of particles. Due to the random distribution of the two DNA strands on the nanoparticle surface in the diconjugate, the observed hexamer structure morphology is not necessarily linear as depicted in the schematic representation. Visual interpretation of these larger particle patterns can be complicated by the variety of angles and ambiguities that arise when two groupings are positioned close together on the grid. For clarity, in Figure 3c we have presented a somewhat narrower field of view in which all of the particle groupings are well-separated.

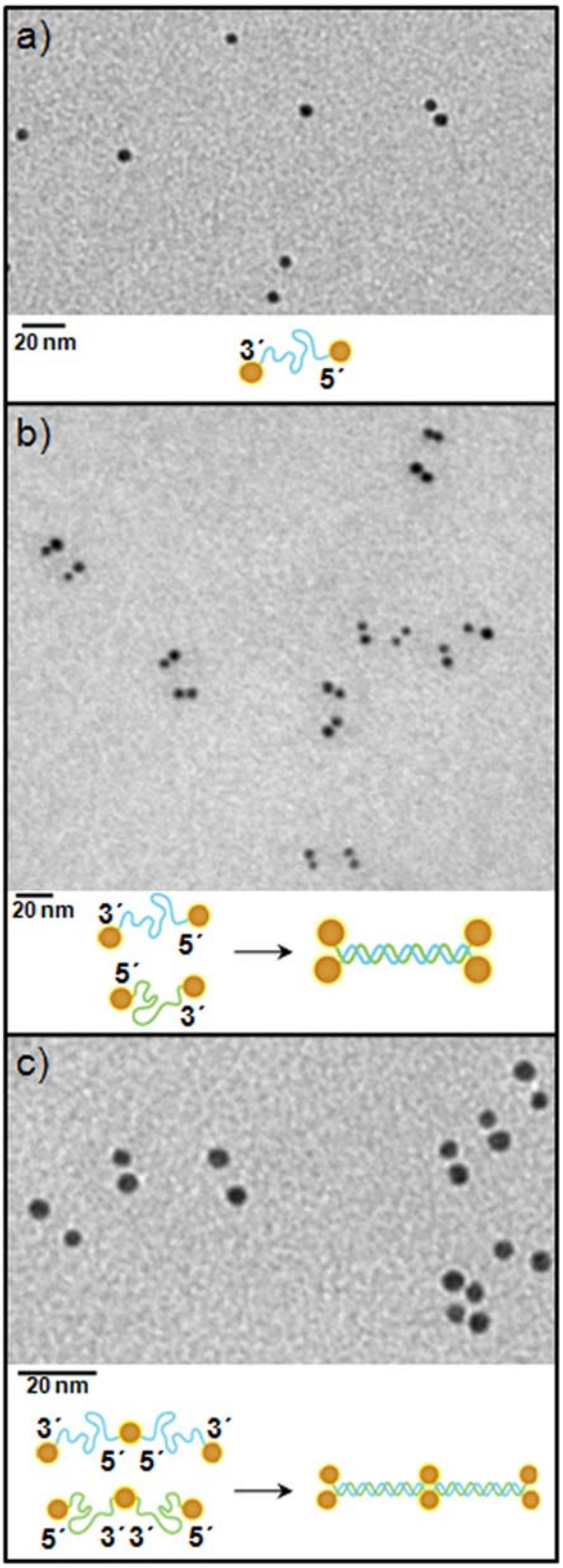

Figure 3. Transmission electron micrographs of ssDNA dimers and trimers hybridized to form larger multi-particle structures: a) ligated 60-base ssDNA dimers; b) complementary ligated dimers hybridized to form nanoparticle tetramers; c) complementary ligated trimers hybridized to form nanoparticle hexamers.

Exponential Amplification of Ligated Nanoparticle Dimers. Polymerase chain reaction (PCR)[11] and ligase chain reaction (LCR)[12] have found wide use as a means of amplifying small amounts of DNA. While PCR has found wider application due to its robustness and ease of use, LCR has also been applied in certain systems as a means of detecting single-nucleotide sequence changes.[12,24] Success in such LCR experiments relies on a careful choice of reaction temperatures[12]: too low a temperature results in reduced selectivity for the desired single-base substitution, while too high a temperature results in a lower amplification efficiency due to DNA melting. We demonstrate the use of nanoparticle monoconjugates as substrates for a ligase chain reaction, amplifying the amount of DNA-gold dimer product formed through repeated thermal cycling in the presence of *Taq* DNA ligase. In these experiments, since our focus is on material construction rather than single-base substitution detection, selectivity constraints do not impact the choice of ligation temperature. Thus we are able to perform ligation at a somewhat lower temperature (chosen as the minimal temperature for good activity of the thermophilic enzyme), resulting in more stable DNA hybridization and presumably therefore in higher reaction efficiencies than we might otherwise achieve.

In this ligase chain reaction (Scheme 3), two strands of DNA are first hybridized to a complementary DNA template to form a nicked double helix. The reaction mixture is then incubated at a moderate temperature (45 °C) to allow the *Taq* DNA ligase enzyme to form a covalent bond at the nick site, and the reaction mixture is subsequently heated to 80 °C to melt the template from the ligated dimer. Since this exceeds the temperature range in which the thiol–gold bond is stable,[25] trithiol terminated DNA is used in synthesizing conjugates to create more strongly bound structures. Following the high-temperature step, the temperature is lowered to 45 °C, which allows the DNA to re-hybridize. In the reaction mixture, conjugates and template halves are initially present in large excess. Thus, although it is possible for a ligated dimer to re-hybridize with a full template, it is statistically more likely that the template will hybridize with conjugate monomers and that the ligated dimer will hybridize with template halves. After the second ligation cycle, assuming 100% ligation efficiency, there will be twice as much ligated dimer. Repeated thermal cycling can then lead to exponential growth in the amount of

ligated dimer product, as 2^n. The amount of dimer present can be monitored by gel electrophoresis (Figure 4a) and plotted against the number of thermal cycles (Figure 4b) to demonstrate exponential growth.

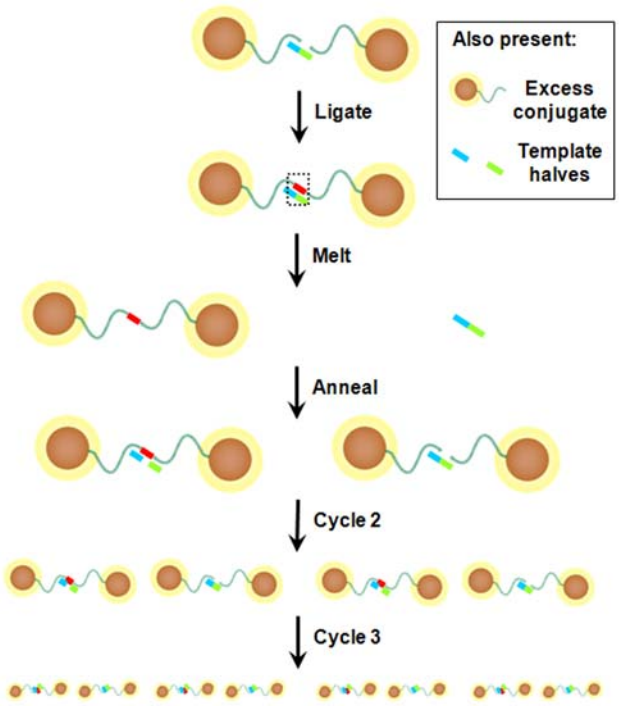

Scheme 3. Amplification of DNA–gold nanostructures via ligase chain reaction (LCR).

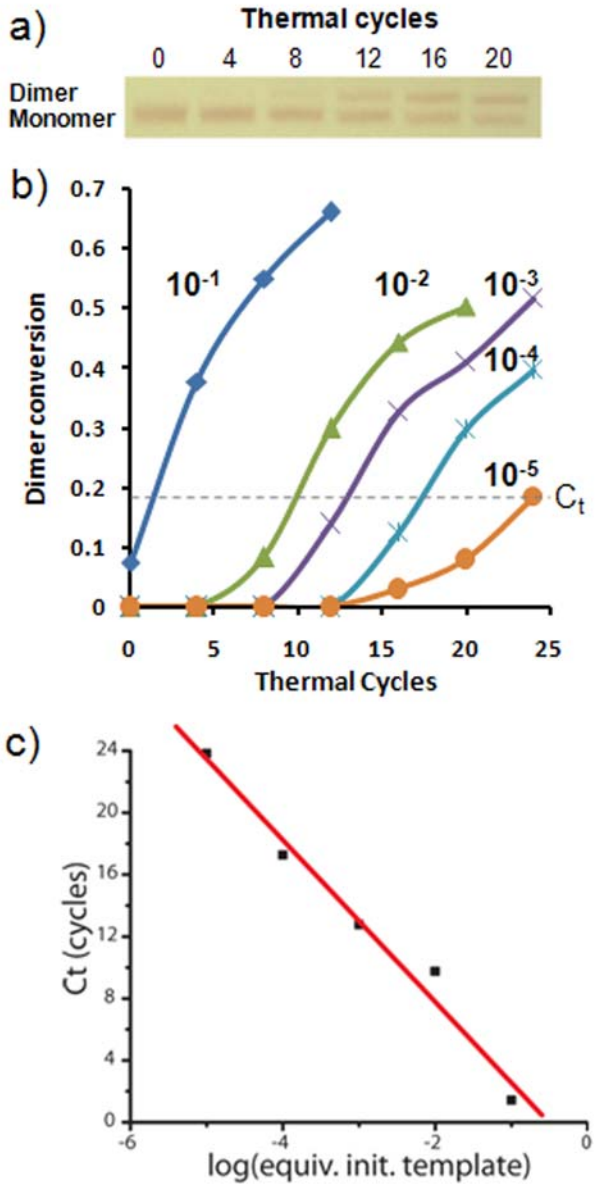

Figure 4. (a) Gel demonstrating exponential conversion of conjugate to dimer with increasing numbers of thermal cycles, starting with 0.01 equiv. template. (b) Graph of conversion to dimer for reactions with different starting equivalents of template strand (0.1 to 0.00001 equiv.) for increasing numbers of thermal cycles. (c) Plot of log initial template concentration vs number of cycles required to reach 20% conversion to dimer.

In practice, ligation efficiency is less than 100%, both in DNA–only experiments performed by others,[12] and in the nanoparticle conjugate experiments described here. The reaction efficiency can be calculated by plotting the log of the initial template concentration against the number of thermal cycles required to reach a certain percentage conversion. The conversion percentage used can be arbitrarily chosen within the range in which changes can be easily measured, but before the reaction reaches

saturation. Here a conversion percentage of 18% was used. Plotting the data in this fashion (Figure 4c) results in a best-fit line with a slope (m) of -5.3 ± 0.5 cycles/log([template]) which may then be used to calculate the reaction efficiency (E) using the equation $E = 10^{-1/m} - 1$, resulting in an efficiency of 55%. While the gel assay used to measure conversion may result in some counting of unligated conjugates hybridized to a full template, this will not affect the calculated reaction efficiency, which depends upon the slope of the log plot (i.e., the number of thermal cycles separating the curves of the conversion graph in Figure 4c) and not upon the absolute conversion.

Sensitivity is limited by the rate of nonspecific ligation, as is the case for DNA–only LCR experiments. Small amounts of nonspecific ligation are observed after more than 20 thermal cycles, making amplification from less than 10^{-5} equivalents of template impractical. For applications in which sensitivity is critical, a gap-LCR protocol[24] could be adopted, in which conjugates and half-template sequences would be designed to form sticky ends in order to reduce blunt-end ligation.

These enzymatic amplification experiments demonstrate that it is possible to achieve exponential amplification of multi-particle products using a thermal cycling protocol. The experimental protocol used here is intended as a proof-of-concept, since clearly a full equivalent of DNA template could be added in lieu of template halves. However, replacement of the DNA template halves with DNA-gold monoconjugates would result in exponential amplification of two complementary DNA-gold dimer structures from a small amount of template, leading to structures similar to those shown in Figure 3b.

More broadly, this experiment can be considered as a nanoparticle analog of PCR, in which a two-nanoparticle 'sequence' is amplified through repeated thermal cycling. With optimization, such a protocol might provide a route to high-yield syntheses of complex multi-nanocrystal 'sequences' incorporating different types and sizes of nanocrystals, with the precise control over interparticle distance in both the ranges required for plasmon coupling[13,22] and for single-molecule surface-enhanced Raman scattering (SM-SERS).[26]

Even in the absence of such optimization, we expect that the ability to leverage thermal cycling to form discrete multiparticle building blocks in a catalytic fashion from the DNA template will be

valuable as a technique for improving efficiency in nanomaterial construction. Materials scientists have long used thermal annealing to remove defects in materials.[27] Although defects in self-assembled nanoparticle bioassemblies arise in a very different way, the concept of heating and cooling to remove defects is equally applicable to the ligated structures presented here. Melting and rehybridizing would allow 'defects' (unligated and/or unhybridized DNA strands) another opportunity to find and join a ligation partner strand. Correct (ligated) parts of the structure would remain joined through the change in temperature. Thus, the percentage yield of complete product structures would be expected to increase with the number of thermal cycles.

CONCLUSIONS

In these experiments, we have found DNA ligase enzymes to be effective agents for creating covalently linked multi-nanoparticle building blocks capable of self-assembly into complex nanoscale structures. Since the ligated dimers and trimers retain the sequence-specific targeting capability of the ssDNA linker, they can be hybridized in a controlled fashion to yield larger discrete assemblies. These structures are distinct from their dsDNA-linked counterparts when analyzed by SAXS, a feature that could be exploited to study the conformational dynamics of ssDNA in solution. The use of thermostable conjugates and ligase enzymes has also allowed the system to be used to amplify populations of discrete nanoparticle assemblies. Further, since the double-labeled ligation product is analytically distinct from the single-labeled monoconjugate starting materials, DNA–gold conjugates can provide a visual metric for ligation efficiency and could be incorporated into the ligase chain reaction as a readout mechanism. Ongoing experiments seek to leverage these new multi-particle constructs as both self-assembly components and spectroscopic probes.

More broadly, the ability to use DNA-manipulating enzymes on discrete nanoparticle conjugates is potentially very powerful since there are a great number of these enzymes commercially available, each of which performs a very specific operation on its DNA substrate. Many also exhibit sequence specificity, a requirement for DNA modification such as phosphorylation, or a requirement for a

chemical additive such as adenosine triphosphate (ATP) or nicotinamide adenine dinucleotide (NAD). In a materials context, these requirements represent an orthogonal set of internal and external signals which may be used for controlling the step-by-step construction of a functional material.

MATERIALS AND METHODS

General Procedures. Citrate coated 5 nm gold particles with < 10 % deviation in diameter were purchased from Ted Pella (Redding, CA). The bis-(*p*-sulfonatophenyl)phenylphosphine dihydrate dipotassium (BSPP) ligand used to stabilize the nanoparticles in aqueous solutions was obtained from Strem Chemicals (Newburyport, MA). Thiolated poly(ethylene glycol) (PEG), MW=356.5 was purchased from PolyPure (Oslo, Norway). Thiolated DNA purified by polyacrylamide gel electrophoresis (PAGE, was purchased from Integrated DNA Technologies (Coralville, IA); trithiolated PAGE–purified DNA was obtained from Fidelity Sytems (Gaithersburg, MD). DNA was resuspended in deionized water to a working concentration of 50-100 μM. T4 and *Taq* DNA ligases were purchased from New England Biolabs (Ipswich, MA). Nanoparticle sample purification and concentration were carried out in a Fisher Centrific 228 or IEC MicroCL 218 bench top centrifuge. UV-Vis absorption measurements were taken using a Perkin-Elmer Lambda 35 spectrometer. Thermal cycling was performed in a Bio-Rad (Hercules, CA) PTC-100 thermal cycler. SAXS data were collected using a Bruker (Madison, WI) Nanostar Small Angle Spectrometer with a Bruker HiStar two-dimensional gas filled detector, using samples sealed in 2mm quartz capillaries purchased from Charles-Supper (Natick, MA).

Transmission electron microscopy was performed using a Phillips Tecnai G^2 20 instrument. Carbon-coated copper TEM grids (Ted Pella) were ionized for 30 s in a Harrick Plasma PDC-32G oxygen plasma cleaner to increase surface hydrophilicity, then 0.5 μL of dilute aqueous sample was spotted on the surface. The sample was left on the grid for 3 minutes to allow particles to adsorb to the surface before adding 10 μL of 0.5X Tris-Borate-EDTA (TBE) buffer and touching the edge of the grid with a filter paper to wick off excess moisture and salts. Buffer addition and wicking were repeated two more times. Grids were then allowed to air dry prior to analysis.

DNA Sequences.

Table 1 shows the sequences of the DNA strands used in ligation-templated self-assembly experiments and exponential amplification experiments. Sequences ampA and ampB were purchased from Fidelity Systems with double polyacrylamide gel electrophoresis (PAGE) purification. All other sequences were purchased from IDT with either PAGE or high performance liquid chromatography (HPLC) purification. The trithiol modifier used in sequence ampA is the linker originally described by Letsinger.[28]

Table 1. DNA sequences used for ligation experiments.

Name	Description	Sequence
A	ligation conjugate strand 1	5′– HS – $(CH_2)_6$ – ATC GAT GCG ATT AAA GGA TGC CTG AGA GCG – 3′
B	ligation conjugate strand 2	5′– H_2PO_4 – CCG AGG TGT CCA CAT AAA GGT GAG ATC CTG – $(CH_2)_3$ – SH – 3′
B_c	ligation conjugate strand 2 complement	5′– HS – $(CH_2)_6$ – CAG GAT CTC ACC TTT ATG TGG ACA CCT CGG – 3′
A_c	ligation conjugate strand 1 complement	5′– H_2PO_4 – CGC TCT CAG GCA TCC TTT AAT CGC ATC GAT – $(CH_2)_3$ – SH – 3′
nA_cB_cn	ligation template	5′– GGG AGT ACT ACG ATG TGG ACA CCT CGG CGC TCT CAG GCA TCC AGA ACT ATT CCG – 3′
n_cABn_c	ligation template complement	5′– CGG AAT AGT TCT GGA TGC CTG AGA GCG CCG AGG TGT CCA CAT CGT AGT ACT CCC – 3′
ampA	amplification conjugate strand 1	5′ – Letsinger trithiol – $(T)_{30}$ – GGC GTT GAT GGA ACT ATC GT – 3′
ampB	amplification conjugate strand 2	5′ – H_2PO_4 – GGT GTC TAC TCT GCC GGT AA – $(T)_{30}$ – dithiol dU – $(CH_2)_6$ – SH – 3′
C40	amplification full template	5′– TTA GCG GCA GAG TAG ACA CCA CGA TAG TTC CAT CAA CGC C – 3′
C40_1	amplification half template 1	5′– H_2PO_4 – ACG ATA GTT CCA TCA ACG CC – 3′
C40_2	amplification half template 2	5′– GGC GTT GAT GGA ACT ATC GT – 3′

Synthesis of Gold–DNA Conjugates. Gold samples were prepared following a literature procedure, described briefly here.[10] To 100 mL of citrate coated 5 nm gold nanoparticle solution, 60 mg of bis-(*p*-sulfonatophenyl)phenylphosphine dihydrate dipotassium salt was added, and the mixture was stirred at

room temperature in order to allow phosphine ligands to replace the citrate ligands. Following overnight incubation, NaCl was added to the stirring mixture until a color change from red to cloudy purple was observed. The solution was transferred to 50 mL centrifuge tubes and centrifuged at room temperature for 10 min at 3500 rpm to collect the precipitated gold. The supernatant was removed, and the pellet re-suspended in phosphine buffer (1 mg of BSPP in 1 mL of de-ionized water), to a final nanoparticle concentration of approximately 3 μM. Nanoparticles and Au–DNA conjugates were quantified by measuring the absorbance at λ = 520 nm and calculating the concentration using Beer's law based on their extinction coefficients: $\varepsilon_{520}(5\text{ nm}) = 9.3 \times 10^6\ M^{-1}cm^{-1}$.

To prepare Au–DNA conjugates, 5′-thiolated DNA was mixed with concentrated gold colloid and 1/8 volume phosphine buffer (1 mg BSPP in 20 μL ddH_2O) and 1/8 volume 20 mM phosphate buffered saline (PBS), pH 7.4. In a typical experiment, 80 μL of gold colloid was mixed with 10 μL of phosphine buffer and 10 μL of PBS and the appropriate volume of DNA (usually about 5 μL). The mixture was incubated with gentle agitation at room temperature for 4 – 24 h, then 1/5 volume PEG solution (1 μL thiolated PEG in 50 μL ddH_2O) was added and the solution was incubated with gentle agitation for a further 2 h.

AE-HPLC of DNA–Au Conjugates. Monoconjugates were purified using an anion-exchange chromatography method published previously[17] and described briefly here. Conjugates were separated using a Dionex DNA-Pac PA100 anion exchange column (Sunnyvale, CA) on an Agilent 1100 series HPLC with in-line degasser, autosampler, multi-wavelength UV-Vis detector, and fluorescence detector. Fractions were collected using an Agilent 1200 series automatic fraction collector. In a typical separation, 100 μl of conjugate prepared as described above was injected using an autosampler and an initial mobile phase composed of 25 mM Tris (pH 8) and 40 mM NaCl in deionized water. The low ionic strength in the mobile phase was maintained for 3 minutes to encourage strong binding of the sample to the column. Subsequently the NaCl concentration was increased from 40 mM to 900 mM over a period of 20 minutes. Sample elution was detected by monitoring UV-Vis absorption at the gold plasmon maximum of 520 nm against a reference of 850 nm, at which the gold colloid does not absorb.

Automatic fraction collection was also triggered by monitoring these wavelengths. In these experiments the monoconjugate (second peak, typically at or around 12 minutes) and diconjugate (third peak, at or around 13 minutes) were collected. It should be noted that the unconjugated gold peak sometimes spans the 40 mM threshold; thus it is possible for the peak to split, resulting in one peak eluting immediately (< 1 min), and one shortly after the sodium chloride concentration begins to increase (at or around 5 minutes). Collected fractions were concentrated either in Centricon 50k MWCO centrifugal filters, or pelleted by high-speed centrifugation (60 min at 14800 rpm) prior to use in hybridization experiments. Typical final concentrations for collected conjugates were 0.2 – 1.5 μM.

T4 DNA Ligation Buffer. Since standard T4 DNA ligase buffer contains dithiothreitol (DTT), which was found to precipitate gold nanoparticles, a modified buffer was prepared without DTT. **(**5 mmol) Tris-HCl and (1 mmol) $MgCl_2$ were dissolved in deionized water to a volume of 9 mL and brought to pH 7.5 by addition of a concentrated solution of NaOH. The solution was stored frozen. Immediately prior to use in ligation experiments, buffer was thawed and 1/9 volume 100 mM ATP (in deionized H_2O at pH 7.5) was added to the volume of buffer to be used in the experiment.

***Taq* DNA Ligation Buffer.** Since standard *Taq* DNA ligation buffer contains DTT and the detergent TritonX-100, which were found to precipitate gold nanoparticles, a modified buffer was prepared without these reagents. (2 mmol) Tris-HCl, (2.5 mmol) potassium acetate, and (1 mmol) magnesium acetate were dissolved in deionized water to a final volume of 9 mL and brought to pH 7.6 by addition of a concentrated solution of NaOH. The solution was stored frozen. Immediately prior to use in thermal cycling experiments, buffer was thawed and 1/9 volume 100 mM nicotinamide adenine dinucleotide (NAD) (in deionized water at pH 7.6) was added to the volume of buffer to be used in the experiment.

Ligation of DNA–Au Conjugates. Concentrated conjugates as described above were hybridized with equimolar quantities of templates and partner conjugates to create gold nanoparticle dimers. In a typical experiment, 2 pmol each of 5 nm monoconjugates A and B and the template DNA strand nA_cB_cn were mixed, vortexed briefly, inserted in a heat block at 45 °C, and left to cool slowly to room temperature for at least 2 hours or as long as overnight. Since conjugates purified by AE-HPLC are isolated in a

high-salt buffer, no additional sodium chloride was added in the hybridization step. To the hybridized mixture, 1/9 volume T4 ligase buffer and 1/19 volume T4 DNA ligase were added. The mixture was vortexed briefly and incubated at 16 °C for 30 minutes.

Removal of Ligation Template. Following ligation, the template complement strand n_cABn_c was added. In a typical reaction, 1 pmol template complement was added per 1 pmol of template. The reaction was mixed thoroughly and placed in a heat block at 50 °C then allowed to cool slowly on the bench top to room temperature (at least 2 hours or as long as overnight).

Enzymatic Amplification of DNA–Au Conjugate Structures. Concentrated monoconjugates ampA and ampB as described above were mixed with varying substoichiometric amounts of template strand C40 and stoichiometric amounts of half-template strands C40_1 and C40_2, then subjected to thermal cycling in the presence of *Taq* DNA ligase to induce enzymatic amplification. In a typical experiment, 10 pmol each of 5 nm monoconjugates ampA and ampB were mixed with 0.01 pmol template and 10 pmol each half-template with deionized water added to reach a volume of 85 μL. Addition of 5 μL *Taq* DNA ligase and 10 μL *Taq* ligase buffer (described above) brought the total reaction volume to 100 μL. The mixture was vortexed to ensure thorough mixing, then split into five 20-μL aliquots, which were subjected to 4, 8, 12, 16, and 20 thermal cycles. Each thermal cycle comprised a 15-min ligation period at 45 °C followed by a 1-min melting period at 80 °C. Samples which were subjected to smaller numbers of thermal cycles were held at room temperature after cycling until all samples were finished. Following thermal cycling, reaction products were analyzed by gel electrophoresis.

Electrophoresis of Au–DNA Hybrid Structures. Gels were prepared with 3% agarose by weight in 0.5X TBE buffer. Samples were diluted with 1/5 volume 3X loading buffer containing 15% Ficoll 400 (Fluka, Milwaukee, WI) and then loaded into the appropriate well. Gels were run at 10 V/cm for 45 min and visualized over white light using a Nikon D1x digital SLR camera.

Small Angle X-ray Scattering Experiments. Nanoparticle dimer samples for SAXS were prepared with 15 pmol of DNA–gold conjugates hybridized with template to yield approximately 7.5 pmol of dimers in a volume of 20 μL. Each sample was sealed in a quartz capillary with a diameter of 2 mm.

The X-ray source was a copper tube for which $\lambda = 1.54$Å. The primary beam was collimated with pinholes to a 400 μm diameter spot. Measurements were performed using a two-dimensional gas filled detector, with a diameter of 11.5 cm and a sample to detector distance of 105 mm. Under these conditions the maximum scattered 2θ angle measurable was 3.0°. Scattered intensity was measured in terms of the scattering vector q. Given the presence of a 2.0 mm beam stop, and the finite size of the detector, the measured q range was from 0.013 $Å^{-1}$ to 0.213 $Å^{-1}$.

Each sample was probed for 18000 s. The temperature in the experiment was estimated by sealing a thermocouple into a capillary containing a typical gold nanoparticle solution and measuring the temperature over the course of the scan. The average temperature was 20.1 °C, and varied less than 0.5 °C over five hours of X-ray illumination.

The raw SAXS data, I(q) vs q, clearly show the presence of a structure factor indicative of proximal nanoparticles, however in reciprocal space it is difficult to observe the length scales present in the sample. Analytical expressions exist to transform the data between reciprocal space data, I(q), and real space pair distribution functions, p(r). However, the transformation from I(q) to p(r) is not generally possible as it requires integration over all q, whereas here only a finite range is measured. Thus the q-space data were transformed into pair distribution functions via the Generalized Indirect Fourier Transformation (GIFT) method using the program GNOM.[29] This algorithm defines the pair distribution function over r as a set of spline functions with linear coefficients, then transforms their sum into q space data. This is possible because p(r) is bounded over a finite range. The transformed pair distribution function is compared to the experimental scattering data to solve for the coefficients of the spline functions.

The pair distribution functions show two peaks. The first peak arises from scattering within a single nanoparticle, the second from scattering between the two particles in a dimer. The positions of the peaks indicate, in our case, whether the dimer is joined by a relatively floppy or stiff linker.

ACKNOWLEDGMENT Financial support of this work by the Biomolecular Program of LBNL, U.S. Department of Energy under Contract No. DE-AC02-05CH11231 is acknowledged with thanks. S.A.C. gratefully acknowledges an NSF-IGERT Predoctoral Fellowhsip.

SUPPORTING INFORMATION PARAGRAPH (Word Style "TE_Supporting_Information"). Raw SAXS data.

REFERENCES (Word Style "TF_References_Section").

REFERENCES

(1) Alivisatos, A. P.; Johnsson, K. P.; Peng, X. G.; Wilson, T. E.; Loweth, C. J.; Bruchez, M. P.; Schultz, P. G. *Nature* **1996**, *382*, 609-611.

(2) Katz, E.; Willner, I. *Angewandte Chemie-International Edition* **2004**, *43*, 6042-6108.

(3) Niemeyer, C. M. *Angewandte Chemie-International Edition* **2001**, *40*, 4128-4158.

(4) Voet, D.; Voet, J. G. *Biochemistry*; 2 ed.; John Wiley and Sons, Inc.: New York, 1995.

(5) Kanaras, A. G.; Wang, Z. X.; Brust, M.; Cosstick, R.; Bates, A. D. *Small* **2007**, *3*, 590-594.

(6) Kanaras, A. G.; Wang, Z. X.; Bates, A. D.; Cosstick, R.; Brust, M. *Angewandte Chemie-International Edition* **2003**, *42*, 191-+.

(7) Pena, S. R. N.; Raina, S.; Goodrich, G. P.; Fedoroff, N. V.; Keating, C. D. *Journal of the American Chemical Society* **2002**, *124*, 7314-7323.

(8) Kanaras, A. G.; Wang, Z. X.; Hussain, I.; Brust, M.; Cosstick, R.; Bates, A. D. *Small* **2007**, *3*, 67-70.

(9) Xu, X. Y.; Rosi, N. L.; Wang, Y. H.; Huo, F. W.; Mirkin, C. A. *Journal of the American Chemical Society* **2006**, *128*, 9286-9287.

(10) Loweth, C. J.; Caldwell, W. B.; Peng, X. G.; Alivisatos, A. P.; Schultz, P. G. *Angewandte Chemie-International Edition* **1999**, *38*, 1808-1812.

(11) Saiki, R. K.; Gelfand, D. H.; Stoffel, S.; Scharf, S. J.; Higuchi, R.; Horn, G. T.; Mullis, K. B.; Erlich, H. A. *Science* **1988**, *239*, 487-491.

(12) Barany, F. *Proceedings of the National Academy of Sciences of the United States of America* **1991**, *88*, 189-193.

(13) Sonnichsen, C.; Reinhard, B. M.; Liphardt, J.; Alivisatos, A. P. *Nature Biotechnology* **2005**, *23*, 741-745.

(14) Zanchet, D.; Micheel, C. M.; Parak, W. J.; Gerion, D.; Alivisatos, A. P. *Nano Letters* **2001**, *1*, 32-35.

(15) Sambrook, J.; Russell, D. W. In *Molecular Cloning: A Laboratory Manual*; 3 ed.; Argentine, J., Ed.; Cold Spring Harbor Laboratory Press: New York, 2001; Vol. 1.

(16) Weiss, J. *Handbook of Ion Chromatography*; Wiley: Darmstadt, 2004; Vol. 1.

(17) Claridge, S. A.; Liang, H. W.; Basu, S. R.; Frechet, J. M. J.; Alivisatos, A. P. *Nano Letters* **2008**, *8*, 1202-1206.

(18) Takahashi, M.; Yamaguchi, E.; Uchida, T. *Journal of Biological Chemistry* **1984**, *259*, 41-47.

(19) Engler, M. J.; Richardson, C. C. *The Enzymes*; Academic Press: San Diego, 1982; Vol. 5.
(20) Zanchet, D.; Micheel, C. M.; Parak, W. J.; Gerion, D.; Williams, S. C.; Alivisatos, A. P. *Journal of Physical Chemistry B* **2002**, *106*, 11758-11763.
(21) Park, S. J.; Lazarides, A. A.; Storhoff, J. J.; Pesce, L.; Mirkin, C. A. *Journal of Physical Chemistry B* **2004**, *108*, 12375-12380.
(22) Reinhard, B. M.; Sheikholeslami, S.; Mastroianni, A.; Alivisatos, A. P.; Liphardt, J. *Proceedings of the National Academy of Sciences of the United States of America* **2007**, *104*, 2667-2672.
(23) Bustamante, C.; Bryant, Z.; Smith, S. B. *Nature* **2003**, *421*, 423-427.
(24) Abravaya, K.; Carrino, J. J.; Muldoon, S.; Lee, H. H. *Nucleic Acids Research* **1995**, *23*, 675-682.
(25) Schessler, H. M.; Karpovich, D. S.; Blanchard, G. J. *Journal of the American Chemical Society* **1996**, *118*, 9645-9651.
(26) Bidault, S.; de Abajo, F. J. G.; Polman, A. *Journal of the American Chemical Society* **2008**, *130*, 2750-+.
(27) Callister, W. D. *Materials Science and Engineering: An Introduction*; John Wiley and Sons, Inc.: New York, 2000.
(28) Li, Z.; Jin, R. C.; Mirkin, C. A.; Letsinger, R. L. *Nucleic Acids Research* **2002**, *30*, 1558-1562.
(29) Svergun, D. I. *Journal of Applied Crystallography* **1992**, *25*, 495-503.

SYNOPSIS TOC (Word Style “SN_Synopsis_TOC”).

Enzymatic ligation of discrete nanoparticle–DNA conjugates creates nanoparticle dimer and trimer structures in which the nanoparticles are linked by single-stranded DNA, rather than double-stranded DNA as in previous experiments. Ligation is verified by agarose gel and small-angle X-ray scattering. This capability is utilized in two ways: first to create a new class of multiparticle building blocks for nanoscale self-assembly; second to create a system which can amplify a population of discrete nanoparticle assemblies.

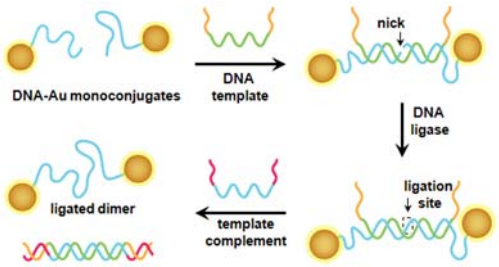

DISCLAIMER